PHYSICAL REVIEW D **92,** 074015 (2015)

Probing the anomalous FCNC top-Higgs Yukawa couplings at the Large Hadron Electron Collider

Wei Liu,[1] Hao Sun,[1,2,*] XiaoJuan Wang,[1] and Xuan Luo[1]

[1]*Institute of Theoretical Physics, School of Physics and Optoelectronic Technology, Dalian University of Technology, No. 2 Linggong Road, Dalian, Liaoning 116024, People's Republic of China*

[2]*LAPTh, Université de Savoie et CNRS, BP110, F-74941 Annecy-le-Vieux Cedex, France*

(Received 4 February 2015; published 12 October 2015)

In this paper, we study the anomalous flavor changing neutral current Yukawa interactions between the top quark, the Higgs boson, and either an up or charm quark ($tqH, q = u, c$). We probe these couplings in $e^- p \to \nu_e \bar{t} \to \nu_e H \bar{q}$ and the channel $e^- p \to \nu_e H b$. Both channels are induced by charged current interactions through $e^- p$ collision at the Large Hadron Electron Collider (LHeC). We study the signatures with the Higgs decay modes $H \to \gamma\gamma, b\bar{b}$ and $\tau^+\tau^-$. Our results show that the flavor changing couplings κ_{tqH} can be probed down to a value of 0.0162 in $e^- p \to \nu_e \bar{t} \to \nu_e H \bar{q}$ with $H \to b\bar{b}$ at a 14 TeV LHeC with a 150 GeV electron beam and 200 fb^{-1} luminosity. This value of the coupling corresponds to the branching ratio $\text{Br}(t \to qH) = 1.34 \times 10^{-4}$.

DOI: 10.1103/PhysRevD.92.074015 PACS numbers: 14.65.Ha, 12.60.-i

I. INTRODUCTION

The discovery of the Higgs boson at the Large Hadron Collider (LHC) [1,2] is a major step towards understanding the electroweak symmetry breaking mechanism and marks a new era in particle physics. In order to ultimately establish the nature of the Higgs boson, a precise measurement of the Higgs couplings to fermions and gauge bosons as well as the Higgs self coupling is needed. These precision measurements will be some of the most important tasks for experiments at the LHC and the future colliders. According to the analyses of the ATLAS and CMS collaborations, the couplings of the Higgs boson have been measured with an overall precision of about 15%, which means that there still remains some room for the existence new physics. Besides the Higgs boson, the measurement of the top quark properties is also important. It is the heaviest known elementary particle, which makes it an excellent candidate for new physics searches. To probe new physics through the Higgs boson and top quark, the top-Higgs Yukawa couplings are of special interest since they are sensitive to new flavor dynamics beyond the standard model (SM) not too far above the electroweak scale. Furthermore, the top quark, as the heaviest SM fermion, owns the strongest Yukawa coupling. Among the Higgs couplings to quarks, the most promising places to reveal new physics at high energy colliders are processes involving top quarks.

The mass of the top quark is heavier than that of the observed Higgs boson, which makes the top quark flavor changing neutral current (FCNC) processes $t \to qH (q = u, c)$ kinematically accessible. In the SM, processes that are induced by FCNC in top quark production or decay are extremely suppressed by the Glashow-Iliopoulos-Maiani mechanism [3] according to SM computation, with decay rates of the order of 10^{-10} or below. However, new physics scenarios, such as the minimal supersymmetric model with/without R-parity violating [4–11], two-Higgs-doublet model [12–15], warped extra dimensions [16,17], alternative left-right symmetric models [18], little Higgs with T parity [19], etc., could enhance the FCNC rates by several orders of magnitude, thus making them detectable using current experimental data. Therefore, studying the top-Higgs FCNC interactions is important both from a theoretical as well as an experimental perspective.

Up to now, the searches for $t \to qH$ have been investigated experimentally at the LHC, which gives the strong limits on the top-Higgs FCNC couplings. Among them, the most stringent constraint of $\text{Br}(t \to cH) < 0.56\%$, $\text{Br}(t \to uH) < 0.45\%$ at 95% confidence level (C.L.) was reported by the CMS collaboration from a combination of the multilepton channel and the diphoton plus lepton channel [20]; while an upper limit is set on the $t \to cH$ branching ratio of 0.79% at the 95% confidence level by the ATLAS collaboration [21,22]. Except for the widely studied $t \to qH$ decays, the importance of the single top Higgs associated production has also been emphasized in the recent theoretical studies especially at the LHC [23–32]. In this paper, we study the anomalous FCNC Yukawa interactions between the top quark, the Higgs boson, and either an up or charm quark ($tqH, q = u, c$) at the Large Hadron Electron Collider (LHeC). The LHeC kinematic range exceeds HERA's by a factor of about 20, due to the combination of a 7 TeV or higher proton beam from the LHC and a new 60 to 150 GeV electron beam. Its

*Corresponding author.
haosun@mail.ustc.edu.cn; haosun@dlut.edu.cn

luminosity is projected to be as high as possibly 10^{34} cm^{-2} s^{-1}, with a default design value of 10^{33} cm^{-2} s^{-1}. This is almost a thousand times higher than HERA's luminosity, which gives the LHeC the potential of a precision measurement Higgs production facility and enables a very large variety of new measurements and searches to be conducted. Typically, we choose two channels to study the anomalous FCNC Yukawa interactions at the LHeC. One is the channel $e^- p \to \nu_e \bar{t} \to \nu_e H \bar{q}$ with $q = u, c$ and the other is the channel $e^- p \to \nu_e H b$. Both channels are charged current (CC) interaction processes induced through $e^- p$ collision at the LHeC.

Our paper is organized as follows: we build the calculation framework in Sec. II including a brief introduction to the anomalous flavor changing tqH couplings and our selected production channels. Section III is arranged to present the numerical results as well as the signal and background analysis. Typically, the $H \to \gamma\gamma, b\bar{b}, \tau^+\tau^-$ decay modes are taken into account. In Sec. IV we present bounds on anomalous tqH couplings at the future LHeC. Finally, we summarize our conclusions in the last section.

II. CALCULATION FRAMEWORK

A. Flavor changing *tqH* couplings

Considering the FCNC Yukawa interactions, the SM Lagrangian can be extended simply by allowing the following terms,

$$\mathcal{L} = \kappa_{tuH} \bar{t} u H + \kappa_{tcH} \bar{t} c H + \text{H.c.}, \tag{1}$$

where the real parameters κ_{tuH} and κ_{tcH} denote the flavor changing couplings of Higgs to up-type quarks. Now we have $m_t - m_h$ larger than m_c, m_u, m_b. In addition to the usual top decay mode $t \to W^{\pm} b$, the top quark can also decay into a charm or up quark associated with a Higgs boson. Therefore, the total decay width of the top-quark Γ_t is

$$\Gamma_t = \Gamma^{\text{SM}}_{t \to W^- b} + \Gamma_{t \to cH} + \Gamma_{t \to uH}. \tag{2}$$

The decay width of the dominant top-quark decay mode $t \to W^- b$ at the leading order (LO) and the next-to-leading order could be found in Ref. [33]. It is given below,

$$\Gamma^{\text{SM}}_{t \to W^- b} = \Gamma_0(t \to W^- b) \left\{ 1 + \frac{2\alpha_s}{3\pi} \left[2 \left(\frac{(1-\beta_W^2)(2\beta_W^2 - 1)(\beta_W^2 - 2)}{\beta_W^4 (3 - 2\beta_W^2)} \right) \ln(1 - \beta_W^2) - \frac{9 - 4\beta_W^2}{3 - 2\beta_W^2} \ln \beta_W^2 + 2\text{Li}_2(\beta_W^2) - 2\text{Li}_2(1 - \beta_W^2) - \frac{6\beta_W^4 - 3\beta_W^2 - 8}{2\beta_W^2 (3 - 2\beta_W^2)} - \pi^2 \right] \right\}, \tag{3}$$

where $\Gamma_0(t \to W^- b) = \frac{G_F m_t^3}{8\sqrt{2}\pi} |V_{tb}|^2 \beta_W^4 (3 - 2\beta_W^2)$ is the LO decay width and $\beta_W = (1 - m_W^2/m_t^2)^{\frac{1}{2}}$ is the velocity of the W boson in the top-quark rest frame. G_F is the Fermi constant. The $t \to u(c)H$ partial decay width is given as [34]

$$\Gamma_{t \to u(c)H} = \frac{\kappa^2_{tu(c)H}}{16\pi} m_t [(\tau_{u(c)} + 1)^2 - \tau_H^2] \times \sqrt{1 - (\tau_H - \tau_{u(c)})^2} \sqrt{1 - (\tau_H + \tau_{u(c)})^2} \tag{4}$$

where $\tau_H = \frac{m_H}{m_t}$, $\tau_{u(c)} = \frac{m_{u(c)}}{m_t}$. The leading order branching ration for $t \to qH$ is then given by

$$\text{Br}(t \to u(c)H) = \frac{\kappa^2_{tu(c)H}}{\sqrt{2} G_F m_t^2} \frac{(1 - m_H^2/m_t^2)^2}{(1 - m_W^2/m_t^2)^2 (1 + 2m_W^2/m_t^2)} \approx 0.512 \kappa^2_{tu(c)H}. \tag{5}$$

Here, the Higgs boson and the top-quark masses are chosen to be $m_H = 125.7$ GeV and $m_t = 173.21$ GeV, respectively. Similar to the top-quark decay, the new interactions affect also the width of the Higgs boson though the additional decay into an off-shell top that subsequently leads to a single W decay of the Higgs boson, namely, $H \to u(c)(t^* \to Wb)$ where t^* denotes off-shell top quark. Therefore, we get

$$\Gamma_H = \Gamma_H^{\text{SM}} + \Gamma_{H \to u(\bar{t}^* \to \bar{b} W^-)} + \Gamma_{H \to \bar{u}(t^* \to b W^+)} + \Gamma_{H \to c(\bar{t}^* \to \bar{b} W^-)} + \Gamma_{H \to \bar{c}(t^* \to b W^+)} \tag{6}$$

where Γ_H^{SM} is the normal Higgs decay width in the SM; while other terms related to the Higgs boson three-body decays are numerically estimated following Ref. [23].

The stringent constraints on the anomalous FCNC couplings are set exploiting the experimental data of the CMS and ATLAS collaborations [20–22]. Theoretically, many other phenomenological studies are performed based on these experimental data. The analysis of Ref. [24] emphasizes the importance of anomalous single top plus Higgs production at the LHC deriving the 95% C.L. upper limits $\text{Br}(t \to cH) < 0.15\%$ and $\text{Br}(t \to uH) < 0.19\%$. Reference [25] studies the single top and Higgs associated production $pp \to tHj$ in the presence of top-Higgs FCNC couplings at the LHC, giving the upper limits as $\text{Br}(t \to qH) < 0.12\%$, $\text{Br}(t \to uH) < 0.26\%$ and $\text{Br}(t \to cH) < 0.23\%$ with an integrated luminosity of 3000 fb^{-1}

at $\sqrt{s} = 14$ TeV. Reference [26] quotes a 95% C.L. limit sensitivity in the $tt \to Wb + hq \to \ell\nu b + \ell\ell(\gamma\gamma)q$ final state of $\mathrm{Br}(t \to qH) < 5(2) \times 10^{-4}$ with an integrated luminosity of 300(3000) fb^{-1} at $\sqrt{s} = 14$ TeV. As can be seen the upper limits on the flavor changing top quark decays can be significantly improved as expected at a high luminosity LHC. Reference [27] derives model-independent constraints on the tcH and tuH couplings that arise from the bounds on hadronic electric dipole moments. References [28,29] study the top-quark decay into Higgs boson, a light quark, and top Higgs associated production including the next-to-leading order QCD effects. Other related publications can be found, for example, in Refs. [30–32,35], etc.

B. The processes

Now we turn to study the selected production processes where the effect of the flavor changing couplings could be significant.

1. $e^- p \to \nu_e \bar{t} \to \nu_e H \bar{q}$ channel

The first channel we consider is $e^- p \to \nu_e \bar{t} \to \nu_e H \bar{q}$ production. The parton level signal process at the LHeC can be expressed as

$$e^-(p_1) + \bar{b}(p_2) \to \nu_e + \bar{t} \to \nu_e(p_3) + H(p_4) + \bar{q}(p_5) \qquad (7)$$

with $q = u, c$ and p_i being the four-momentum of initial and final particles, respectively. The Feynman diagram for the partonic process is depicted in Fig. 1. The flavor changing vertex proportional to the flavor changing coupling κ_{tqH} occurs via the single top production with its following decay to Higgs plus u or c quark, where this single top quark is induced by the collision of b quark from the proton with the W^- boson emission from the electron beam. We thus expect the cross sections for these processes to be proportional to $c\kappa_{tqH}^2$ where c is some related constants. The parent level signal process $e^- p \to \nu_e H \bar{q} + X$, the kinematic distributions, and integrated cross sections can then be obtained by convoluting the parton level process with the parton distribution function (PDF) [36] of quark in the proton,

$$d\sigma(e^- p \to \nu_e H \bar{q} + X) = \int dx G_{\bar{b}/P}(x, \mu_f) d\hat{\sigma}(e^- \bar{b} \to \nu_e \bar{t} \to \nu_e H \bar{q}, \sqrt{\hat{s}}), \qquad (8)$$

where $\sqrt{\hat{s}} = 2\sqrt{x E_e E_p}$ is the center-of-mass (c.m.) colliding energy and x is the momentum fraction of anti-b quark from proton.

2. $e^- p \to \nu_e H b$ channel

The second channel we considered is $e^- p \to \nu_e H b$ production. The parton level signal process at the LHeC can be expressed as

$$e^-(p_1) + q(p_2) \to \nu_e(p_3) + H(p_4) + b(p_5). \qquad (9)$$

The Feynman diagram for the partonic process is depicted in Fig. 2. The FCNC top-Higgs Yukawa couplings are deduced from the initial state $u(c)$-quarks from the proton collision with the anti-top quark from the Wtb coupling. Similarly, the parent level signal process $e^- p \to \nu_e H b + X$ is present as

$$d\sigma(e^- p \to \nu_e H b + X) = \int dx G_{q/P}(x, \mu_f) d\hat{\sigma}(e^- q \to \nu_e H b, \sqrt{\hat{s}}) \qquad (10)$$

where $q = u, c$ and $\sqrt{\hat{s}}$ is again the c.m. colliding energy at the LHeC.

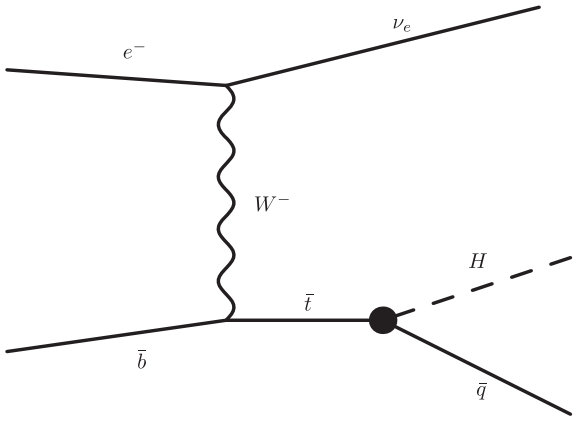

FIG. 1. Partonic Feynman diagrams for $e^- p \to \nu_e \bar{t} \to \nu_e H \bar{q}$ with $q = u, c$. Black blobs represent the anomalous tqH couplings parametrized by Eq. (1).

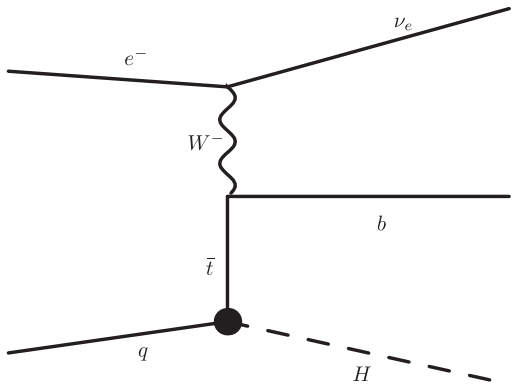

FIG. 2. Partonic Feynman diagrams for $e^- p \to \nu_e H b$. Black blobs represent the anomalous tqH couplings parametrized by Eq. (1).

3. Charged current and neutral current production at the LHeC

The two channels $e^-p \to \nu_e \bar{t} \to \nu_e H\bar{q}$ and $e^-p \to \nu_e Hb$ that we have presented are CC processes where the CC production leads to a top-beauty associated production through W^- boson emission from the initial electron. In addition to CC production, the flavor changing Yukawa couplings can also be produced through neutral current (NC) productions. In NC it gives rise to pair production of top-antitop quarks from a neutral photon/Z boson emission from the initial electron. A comparison of the cross sections of these CC and NC production channels including the anomalous FCNC top-Higgs Yukawa couplings is presented in Table I. The input parameters and the very basic kinematical cuts will be presented in the following discussion.

From Table I, we see that the largest production is CC $e^-p \to \nu_e \bar{t} \to \nu_e H\bar{q}$ production. For $\kappa_{tuH} = 0.1$ it is more than ten times larger than the sum of the other channels. Different from the CC production that leads to a top-beauty final state, the NC production gives rise to pair produced top-antitop quarks. The NC productions are small, but still sizeable at the LHeC especially when the polarized electron beam is considered. Furthermore, in sharp contrast to the LHC, the absence of pileup, and underlying event effects at the LHeC, high rates of single anti-top production are expected to provide a better insight through these production channels. The rapidity distributions of the Higgs boson through different channels are given in Fig. 3. In our paper, we only consider the CC interactions that dominate over all the other production mechanisms. This includes $e^-p \to \nu_e \bar{t} \to \nu_e H\bar{q}$ and $e^-p \to \nu_e Hb$ channels. Looking at Table I, we also find that the cross section of the former channel is larger than that of the latter one by roughly a factor of 20. At first sight this seems odd, because the transition $e^-p(\bar{b}) \to \nu_e \bar{t} \to \nu_e H\bar{q}$ involves an (anti)bottom-quark PDF, while the transition of $e^-p(q) \to \nu_e Hb$ does not. One is therefore tempted to think that the cross section of $e^-p \to \nu_e \bar{t} \to \nu_e H\bar{q}$ is smaller than that of $e^-p \to \nu_e Hb$. However, this naive assertion is incorrect, because for $e^-p \to \nu_e \bar{t} \to \nu_e H\bar{q}$ the internal (anti)top is exchanged in the s-channel, while in the case $e^-p \to \nu_e Hb$ the top appears in a t-channel exchange. The PDF suppression is thus overcompensated by an on-shell enhancement.

TABLE I. A comparison of the cross sections of CC and NC production channels including the anomalous FCNC top-Higgs Yukawa couplings with $\kappa_{tuH} = 0.1$.

$(\sqrt{s}_{e^-}, \sqrt{s}_p) = (150\ [\text{GeV}], 14\ [\text{TeV}])$	
channels	$\sigma(\kappa_{tuH} = 0.1)$ [fb]
$e^-p \to \nu_e \bar{t} \to \nu_e H\bar{q}$	41.64
$e^-p \to \nu_e Hb$	1.987
$e^-p \to e^- Ht$	0.616
$e^-p \to e^- HqW$	0.901

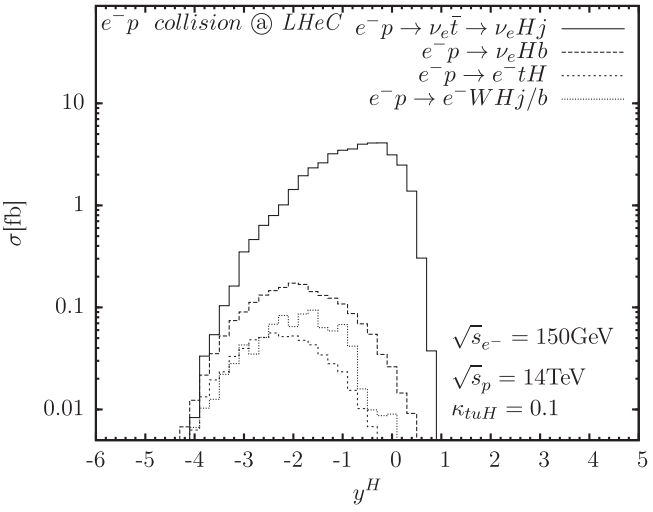

FIG. 3. The rapidity distributions of the Higgs boson through different channels including $e^-p \to \nu_e \bar{t} \to \nu_e H\bar{q}$, $e^-p \to \nu_e Hb$, $e^-p \to e^- Ht$, and $e^-p \to e^- HqW$ productions.

III. RESULTS

A. Input parameters

We take the input parameters as [37] $\alpha_{ew}(m_Z^2)^{-1}|_{\overline{\text{MS}}} = 127.9$, $G_F = 1.166370 \times 10^{-5}\ \text{GeV}^{-2}$, $m_Z = 91.1876$ GeV, so we have $m_W = 79.82436$ GeV and $\sin^2\theta_W = 1 - (m_W/m_Z)^2 = 0.233699$. For the strong coupling constant we take $\alpha_s = 0.1184$. Throughout this paper, we set the quark masses as $m_u = m_d = m_c = m_s = 0$ GeV and $m_b = 4.18$ GeV. The top-quark mass is set to $m_t = 173.21$ GeV with its width $\Gamma_t = 1.3604$ GeV when $\kappa_{tuH} = 0.1$. For the leptons, we keep $m_e = m_\mu = 0$ GeV, and $m_\tau = 1.77682$ GeV. We do not consider the contribution from small CKM matrix $V_{qq'}$ where q and q' are not the same generation. For the mass of the Higgs boson, we take $m_H = 125.7$ GeV with the SM width to be $\Gamma_H^{\text{SM}} = 4.3$ MeV. The partonic cross sections are convoluted with CTEQ6L1 [38] PDFs keeping factorization and renormalization scale $\mu_f = \mu_r = m_t$. For the LHeC colliding energy, we consider the future 14 TeV proton at future LHC and an energetic new electron beam with the energies of 150 GeV [39,40]. The luminosity is taken to be a running parameter. The FCNC couplings are chosen to be $\kappa_{tuH} = 0.1$ and $\kappa_{tcH} = 0$ for simplicity. This set of parameters will be used as the default unless stated otherwise.

B. Kinematic cuts

The event reconstruction is still based on a parametrized, generic LHC-style detector. The general acceptance cuts in the lab frame for the events are

$$
\begin{aligned}
&p_T^{\rm jet} \geq 25\ {\rm GeV}, \quad p_T^b \geq 25\ {\rm GeV}, \quad p_T^\gamma \geq 25\ {\rm GeV},\\
&p_T^\ell \geq 25\ {\rm GeV}, \quad \not{E}_T^{\rm miss} \geq 25\ {\rm GeV},\\
&|\eta^{\rm jet}| < 5, \quad |\eta^b| < 2.5, \quad |\eta^\gamma| < 2.5, \quad |\eta^\ell| < 2.5,\\
&\Delta R(jj) > 0.4, \quad \Delta R(bb) > 0.4, \quad \Delta R(\ell\ell) > 0.4,\\
&\Delta R(\gamma\gamma) > 0.4, \quad \Delta R(\gamma\ell) > 0.4\\
&\Delta R(jb) > 0.4, \quad \Delta R(\ell j) > 0.4, \quad \Delta R(\ell b) > 0.4,\\
&\Delta R(\gamma b) > 0.4, \quad \Delta R(\gamma j) > 0.4
\end{aligned} \tag{11}
$$

where $\Delta R = \sqrt{\Delta\Phi^2 + \Delta\eta^2}$ is the separation in the rapidity-azimuth plane, $p_T^{{\rm jet},\ell,\gamma}$ are the transverse momentum of jets (referred to as j), leptons, and photons while $\not{E}_T^{\rm miss}$ is the missing transverse momentum. We stress here that cuts in Eq. (11) are the very basic ones and might be changed later in the following discussion.

C. Decay modes and backgrounds

1. $e^-p \to \nu_e\bar{t} \to \nu_e H\bar{q}$ channel with $H \to \gamma\gamma(b\bar{b},\tau^+\tau^-)$ decay modes

Let us first consider the $e^-p \to \nu_e\bar{t} \to \nu_e H\bar{q}$ channel with $H \to \gamma\gamma$ decay mode. The considered signal production can be written as

$$e^-p \to \nu_e\bar{t} \to \nu_e H\bar{q} \to \nu_e\gamma\gamma\bar{q} \tag{12}$$

with $q = u, c$. Since in our calculation we take the anomalous FCNC couplings to be $\kappa_{tuH} = 0.1$ and $\kappa_{tcH} = 0$ for simplicity, only $q = u$ contributes. Higgs decays to pairs of photons are simulated using MadGraph [41] where the implementation of the effective $H\gamma\gamma$ interaction is adopted [42]. For simplicity, one can also multiply the production cross sections with the Higgs branching ratio corresponding to the final state. As can be seen, in this case, the studied topology of our signal gives rise to the jet + $\not{E}_T$ + diphoton signature characterized by one jet, a missing transverse momentum ($\not{E}_T$) from the undetected neutrino, and a diphoton signal appearing as a narrow resonance centered around the Higgs boson mass. The irreducible background comes from the SM process $e^-p \to \nu_e\gamma\gamma\bar{q}$, which yields the identical final states with the signal. These backgrounds mainly come from the production of W boson with double photon production through $WW\gamma\gamma$, $W\gamma\gamma$ couplings or through $WW \to H \to \gamma\gamma$ decay associated with jet emission. The others come from jet production associated with emission of photons. In order to obtain the anomalous FCNC tqH coupling effects, we need to simulate all the signal contributions precisely together with these irreducible backgrounds as well as their interference. The total cross section for these reactions thus can be split into three contributions,

$$\sigma = a_0 + a_1\kappa_{tuH} + a_2\kappa_{tuH}^2, \tag{13}$$

where a_0 is the SM prediction, and the term a_1 linear in κ_{tuH} arises from the interference between SM and the anomalous amplitudes, whereas the quadratic term a_2 is the self interference of the anomalous amplitudes. Potentially reducible backgrounds come from various other SM processes that yield different final states that are attributed to the jet + $\not{E}_T$ + diphoton signature due to a misidentification of one or more of the final state objects, for example, two light jets production with both jets faking a diphoton pair, one jet one photon associated production with one jet faking a photon or leptons faking photons, etc. The background arising from $e^-p \to \nu_e\bar{\nu}_e e^-\gamma j$ is smaller than 1 percent of signal after applying all cuts and taking rejection factors into account. We consider all these contributions and take the jet faking a photon rate to be 0.001 and the electron faking photon rate to be 0.062 [43] during data analysis. Although the $\gamma\gamma$ decay channel has a small branching ratio, it has the advantage of good resolution on the $\gamma\gamma$ resonance and is also free from the large QCD backgrounds. Typically, we use a narrow invariant mass window $|m_{\gamma\gamma} - m_H| < 5$ GeV to further reduce the nonresonant backgrounds as well as the jet such that the invariant mass of the $j\gamma\gamma$ system is near the mass of the top quark, say, $m_{j\gamma\gamma}$ belongs to the range $[m_t - 10, m_t + 10]$ GeV.

We define some sets of kinematical cuts as below:

(i) Cut I means the basic cuts present in Eq. (11);
(ii) cut II means the basic cuts plus $25 < \not{E}_T^{\rm miss} < 300$ GeV, $25 < p_T^{\rm jet} < 100$ GeV, $25 < p_T^\gamma < 200$ GeV;
(iii) cut III means cut II plus requiring the invariant mass of the diphoton pair to be in the range $[m_H - 5, m_H + 5]$ GeV;
(iv) cut IV means cut III plus requiring the invariant mass of the diphoton and light jet system to lie in the range $[m_t - 10, m_t + 10]$ GeV.

In Table II, we display the signal and the main background cross sections for $e^-p \to \nu_e\gamma\gamma j$ after the application of cuts I–IV. The rejection factors and the b-tagging effects are already taken into account in this table, where σ_S means the cross section for signal, σ_B for the background. In Fig. 4 we display the signal's and the total background's transverse missing energy ($\not{E}_T^{\rm miss}$) distributions, transverse momentum ($p_T^{\gamma,{\rm jet}}$) distributions, and $\Delta R(\gamma\gamma)$ distributions for $e^-p \to \nu_e\gamma\gamma j$ in parton level after considering cuts I–IV. The anomalous coupling is chosen to be $\kappa_{tqH} = 0.1$. The rejection factors are taken into account. We see that the anomalous FCNC tqH couplings can enhance the SM production to a level where it can be detectable at future LHeC. By a simple fit we get the final cross section to be $\sigma_{\rm total} = 5.10 \times 10^{-5} + 5.21 \times 10^{-5}\kappa_{tuH} + 8.63 \times 10^{-3}\kappa_{tuH}^2$ [pb].

Now we consider the $e^-p \to \nu_e\bar{t} \to \nu_e H\bar{q}$ channel with $H \to b\bar{b}$ decay mode. In this case, the signal production channel is characterized by a missing energy from the

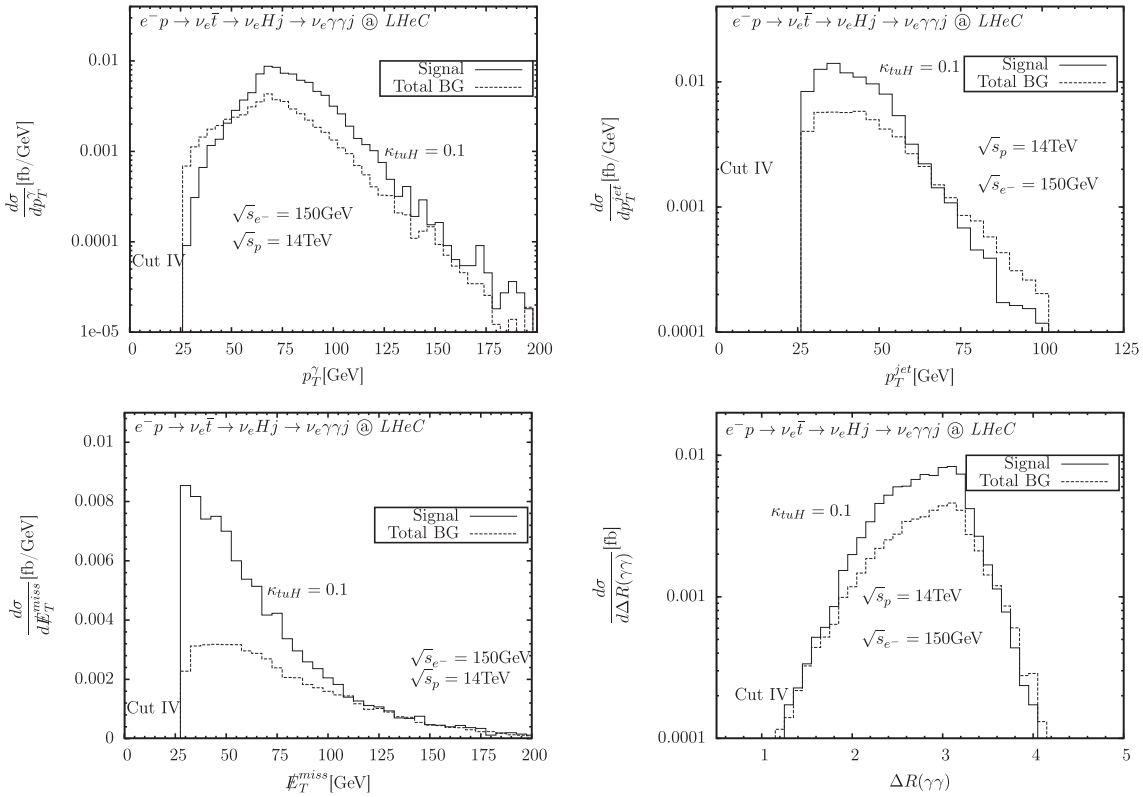

FIG. 4. The signal and total background transverse missing energy ($\not{E}_T^{\rm miss}$) distributions, transverse momentum ($p_T^{\gamma,{\rm jet}}$) distributions, and $\Delta R(\gamma\gamma)$ distributions for $e^- p \to \nu_e \gamma\gamma j$ after considering cuts I–IV. The anomalous coupling is chosen to be $\kappa_{tuH} = 0.1$. The rejection factors are taken into account.

undetected neutrino and a $b\bar{b}$ pair associated with a light jet signal. Still, the $b\bar{b}$ pair signal is appearing as a narrow resonance centered around the Higgs boson mass. The main background processes are $e^- p \to \nu_e b\bar{b} j, bjj, \bar{b}jj$, etc., with light jets faking b jets. In our analysis, we assume a b-jet tagging efficiency of $\epsilon_b = 60\%$ and a corresponding mistagging rate of $\epsilon_{\rm light} = 1\%$ for light jets (u, d, s quark or gluon) and $\epsilon_c = 10\%$ for a c jet, consistent with typical values assumed by the LHC experiments [44].

For this decay mode, we take cuts I–IV to be the same while we take cut II to be the basic cuts plus $25 < \not{E}_T^{\rm miss} < 400$ GeV, $25 < p_T^b < 200$ GeV, $25 < p_T^{\rm jet} < 140$ GeV and $\Delta R(bj) < 4$. For the background production, we also need the special cut for $\nu_e \bar{b} jj$, $\nu_e \bar{b}\, \bar{c}\, j$, etc., with the light jets system not belonging to the range $[m_W - 10, m_W + 10]$ GeV. This cut will not affect the signal much, but it will reduce the background obviously. Finally, we get the signal and total background to be 13 and

TABLE II. Signal and total background cross sections for $e^- p \to \nu_e \bar{t} \to \nu_e H \bar{q}$ channel with different decay modes after the application of cuts I–IV. The rejection factors and b-tagging effects are taken into account in this table.

		Cross sections for $e^- p \to \nu_e \bar{t} \to \nu_e H \bar{q}$ channel ($\kappa_{tuH} = 0.1$)			
Decay	[pb]	Cut I	Cut II	Cut III	Cut IV
$H \to \gamma\gamma$	σ_S	9.31×10^{-5}	9.26×10^{-5}	9.21×10^{-5}	9.04×10^{-5}
	σ_B	2.75×10^{-2}	1.35×10^{-2}	1.02×10^{-3}	5.29×10^{-5}
	S/B	3.39×10^{-3}	6.86×10^{-3}	9.03×10^{-2}	1.71
$H \to b\bar{b}$	σ_S	1.33×10^{-2}	1.33×10^{-2}	1.33×10^{-2}	1.30×10^{-2}
	σ_B	2.65×10^{-1}	1.97×10^{-1}	6.12×10^{-2}	3.02×10^{-3}
	S/B	5.02×10^{-2}	6.75×10^{-2}	2.17×10^{-1}	4.30
$H \to \tau^+\tau^-$	σ_S	2.24×10^{-3}	2.23×10^{-3}	2.23×10^{-3}	2.23×10^{-3}
	σ_B	4.93×10^{-2}	1.87×10^{-2}	6.89×10^{-3}	4.20×10^{-4}
	S/B	4.54×10^{-2}	1.19×10^{-1}	3.24×10^{-1}	5.31

3.02 fb, respectively, and we get the signal background ratio to be 4.3. The final cross section can be written as $\sigma_{\text{total}} = 2.87 \times 10^{-3} + 7.68 \times 10^{-3}\kappa_{tuH} + 1.24\kappa_{tuH}^2$ [pb].

Finally, we consider the $\tau^+\tau^-$ decay mode in this production channel. Our results show that $e^- p \to \nu_e \bar{t} \to \nu_e H \bar{q}$ channel with $H \to \tau^+\tau^-$ decay mode can be another good choice. With the four lists of cuts, we take cuts I–IV to be the same while we take cut II to be the basic cuts plus $25 < \not{E}_T^{\text{miss}} < 300$ GeV, $25 < p_T^j < 100$ GeV, $25 < p_T^\ell < 200$ GeV and $\Delta R(\ell j) < 4$. The total cross section can be parametrized as $\sigma_{\text{total}} = 3.96 \times 10^{-4} + 1.30 \times 10^{-3}\kappa_{tuH} + 2.13 \times 10^{-1}\kappa_{tuH}^2$ [pb]. The cross sections of the above decay modes are presented in Table II with different sets of cuts. We see that the $H \to \gamma\gamma$ decay mode provides the smallest signal since the branching ratio of $H \to \gamma\gamma$ is quite small. By applying the cuts, the background can be reduced to the same level. For the $H \to b\bar{b}, \tau^+\tau^-$ decay modes, the signal can be five times larger than the backgrounds, thus making the signal over background around 5 for κ_{tuH} equal to 0.1. The distributions of the signals and backgrounds are similar to Fig. 4 and we therefore do not display them.

2. $e^- p \to \nu_e H b$ channel with $H \to \gamma\gamma(b\bar{b}, \tau^+\tau^-)$ decay modes

We apply a similar method to $e^- p \to \nu_e H b$ production channel. However, due to the critical large backgrounds, we use much harder cuts instead: For $H \to \gamma\gamma$ decay mode, cut I still means the very basic cuts present in Eq. (11); cut II means cut I plus $|\eta^{\text{jet}}| < 2.5$ GeV, $p_T^b > 100$ GeV, $\Delta R(\gamma j) < 4$ GeV; cut III means cut II plus invariance mass of diphoton pair belonging to $[m_h - 3, m_h + 3]$ GeV; cut IV means cut III plus $p_T^\gamma > 150$ GeV, $p_T^b > 250$ GeV, $\Delta R(\gamma\gamma) < 1.5$ GeV. For $H \to b\bar{b}$ decay mode, we use cut II to be the basic cuts plus $|\eta^{\text{jet}}| < 2.5$ GeV, $\Delta R(\gamma j) < 4$ GeV, and cut IV to be cut III plus $p_T^b > 200$ GeV. For $H \to \tau^+\tau^-$ decay mode, we use cut II to be the basic cuts plus $|\eta^{\text{jet}}| < 2.5$ GeV, $\Delta R(\gamma j) < 4$ GeV, cut IV to be cut III plus $p_T^b > 200$ GeV, $p_T^\ell > 125$ GeV, $\Delta R(\ell\ell) < 1.5$ GeV. When jet fakes b, we replace the cuts for b to jets. In Table III, we display the signal and total background cross sections after the application of cuts I–IV. Here in the table the rejection factors and b-jet tagging efficiency are taken into account.

We see that in order to test the anomalous tqH coupling, the best choice of decay mode through $e^- p \to \nu_e H b$ channel is $H \to b\bar{b}$. Though its cross section is much smaller than that of the one in $e^- p \to \nu_e \bar{t} \to \nu_e H \bar{q}$ channel with associated $b\bar{b}$ decay mode, its signal over background ratio is not small. However, its cross section is small after the critical set of cut IV, which makes the detection a challenge. By a simple fit we get $\sigma_{\text{total}} = 5.41 \times 10^{-9} + 7.43 \times 10^{-9}\kappa_{tuH} + 8.00 \times 10^{-6}\kappa_{tuH}^2$ [pb] for $H \to \gamma\gamma$.$\sigma_{\text{total}} = 1.46 \times 10^{-7} + 1.54 \times 10^{-7}\kappa_{tuH} + 3.43 \times 10^{-4}\kappa_{tuH}^2$ [pb] for $H \to b\bar{b}$. $\sigma_{\text{total}} = 3.68 \times 10^{-7} + 1.86 \times 10^{-7}\kappa_{tuH} + 3.42 \times 10^{-4}\kappa_{tuH}^2$ [pb] for $H \to \tau^+\tau^-$.

D. Data analysis and search sensitivity

We follow Refs. [45,46] exactly to obtain the sensitivity limits. Typically, the limits are achieved by assuming the number of observed events equal to the SM background prediction, $N_{\text{obs}} = \sigma_B \times \mathcal{L} \times \epsilon$, with $\mathcal{L}$ for a given integrated luminosity and ϵ the detection efficiency. σ_B is the cross section of SM background prediction. As can be seen, the SM background events can be less or larger than ten for different values of the luminosity. We thus estimate the sensitivity limits on the anomalous tqH coupling through both channels by using two different statistical analysis methods depending on the number of observed events N_{obs}. For $N_{\text{obs}} \leq 10$, we employ a Poisson distribution method. In this case, the upper limits of number of events N_{up} at the 95% C.L. can be calculated from the formula

$$\Sigma_{k=0}^{N_{\text{obs}}} P_{\text{Poisson}}(N_{up}; k) = 1 - \text{C.L.} \tag{14}$$

TABLE III. Signal and total background cross sections for $e^- p \to \nu_e H b$ channel with different decay modes after the application of cuts I–IV. The rejection factors and the b-tagging effects are taken into account in this table.

		Cross sections for $e^- p \to \nu_e H b$ channel ($\kappa_{tuH} = 0.1$)			
Decay	[pb]	Cut I	Cut II	Cut III	Cut IV
	σ_S	1.66×10^{-6}	1.24×10^{-6}	1.23×10^{-6}	0.80×10^{-7}
$H \to \gamma\gamma$	σ_B	2.70×10^{-4}	5.31×10^{-5}	1.99×10^{-6}	3.32×10^{-9}
	S/B	6.15×10^{-3}	2.34×10^{-2}	6.18×10^{-1}	24.1
	σ_S	2.38×10^{-4}	2.36×10^{-4}	2.16×10^{-4}	3.44×10^{-6}
$H \to b\bar{b}$	σ_B	6.05×10^{-3}	3.14×10^{-3}	1.27×10^{-3}	1.49×10^{-7}
	S/B	3.93×10^{-2}	7.52×10^{-2}	1.70×10^{-1}	23.1
	σ_S	4.01×10^{-5}	3.99×10^{-5}	4.00×10^{-5}	3.41×10^{-6}
$H \to \tau^+\tau^-$	σ_B	5.42×10^{-4}	2.86×10^{-4}	6.44×10^{-5}	2.23×10^{-7}
	S/B	7.40×10^{-2}	1.40×10^{-1}	6.21×10^{-1}	15.3

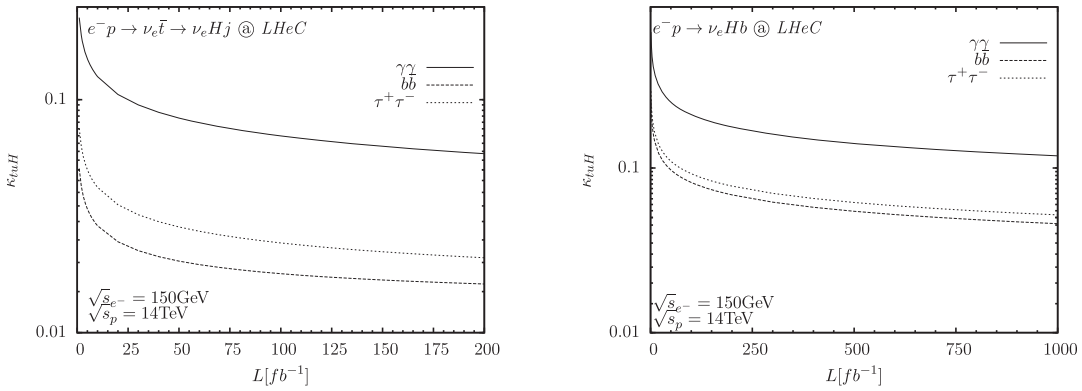

FIG. 5. The contour plots in luminosity-κ_{tuH} plane for expected 95% C.L. limits at 14 TeV LHeC.

Values for limits candidate N_{up} can be found in Ref. [37]. The expected 95% C.L. limits on κ_{tqH} can then be calculated by the limits of the observed cross sections. The integrated luminosity $\mathcal{L}$ will be taken as a running parameter. For $N_{\rm obs} > 10$, a chi-square (χ^2) analysis is performed with the definition

$$\chi^2 = \left(\frac{\sigma_{\rm tot} - \sigma_B}{\sigma_B \delta}\right)^2 \tag{15}$$

where $\sigma_{\rm tot}$ is the cross section containing new physics effects and $\delta = \frac{1}{\sqrt{N}}$ is the statistical error with $N = \sigma_B \times \mathcal{L} \times \epsilon$. The parameter sensitivity limits on anomalous tqH coupling as a function of the integrated luminosity can then be obtained.

In Fig. 5, we plot the contours of expected 95% C.L. limits to κ_{tuH} at 14 TeV LHeC with 150 GeV electron beam for $e^-p \to \nu_e \bar{t} \to \nu_e H\bar{q}$ (left panel) and $e^-p \to \nu_e Hb$ (right panel) channels, respectively. The solid curve, dotted curve, and dashed curve are for $H \to \gamma\gamma$, $H \to b\bar{b}$, $H \to \tau^+\tau^-$ decay modes, respectively. From Fig. 5, we can see that the probed κ_{tuH} limits from $e^-p \to \nu_e \bar{t} \to \nu_e H\bar{q}$ channel are much smaller than those from $e^-p \to \nu_e Hb$ channel. Typically, we get 0.0588, 0.0162, 0.0209 for κ_{tuh} by using $H \to \gamma\gamma$, $H \to b\bar{b}$, $H \to \tau^+\tau^-$ decay modes, respectively, which corresponds to the branching ratio $\mathrm{Br}(t \to qH) = 0.177\%$, $\mathrm{Br}(t \to qH) = 0.0134\%$, $\mathrm{Br}(t \to qH) = 0.0223\%$ at 14 TeV LHeC with 200 fb^{-1} luminosity for the former channel, and 0.177, 0.0701, 0.0776 for the latter, corresponding to the branching ratio $\mathrm{Br}(t \to qH) = 1.604\%$, $\mathrm{Br}(t \to qH) = 0.252\%$, $\mathrm{Br}(t \to qH) = 0.308\%$. Thus, we apply higher luminosity for the latter channel, reaching to 1000 fb^{-1}. Then the research limits change to 0.118, 0.0468, and 0.0518 for κ_{tuH}, which corresponds to 0.713%, 0.112%, 0.137% for the branching ratio. We can see that the LHeC sensitivity to the coupling κ_{tuH} is much improved by using $e^-p \to \nu_e \bar{t} \to \nu_e H\bar{q}$ channel. And for different decay modes, $H \to b\bar{b}$ is the best one for both channels.

TABLE IV. Summary for the expected 95% C.L. limits of $\mathrm{Br}(t \to qH)$ for $e^-p \to \nu_e \bar{t} \to \nu_e H\bar{q}$ and $e^-p \to \nu_e Hb$ channels with $H \to \gamma\gamma$, $H \to b\bar{b}$, and $H \to \tau^+\tau^-$ decay modes at 14 TeV LHeC with 10(200) fb^{-1} luminosity.

	$e^-p \to \nu_e \bar{t} \to \nu_e H\bar{q}$		$e^-p \to \nu_e Hb$	
	$\mathcal{L}$[fb^{-1}]	$\mathrm{Br}(t \to qH)$	$\mathcal{L}$[fb^{-1}]	$\mathrm{Br}(t \to qH)$
$H \to \gamma\gamma$	10	0.813%	10	7.200%
	200	0.177%	200	1.604%
$H \to b\bar{b}$	10	0.0425%	10	1.121%
	200	0.0134%	200	0.251%
$H \to \tau^+\tau^-$	10	0.0899%	10	1.377%
	200	0.0223%	200	0.312%

In Table IV, we give the $\mathrm{Br}(t \to qH)$ for different decay modes for both channels at 14 TeV LHeC with 10(200) fb^{-1} luminosity, respectively. We see that the limits have improved by almost four times when the luminosity increases from 10 to 200 fb^{-1}. When comparing different decay modes, $H \to b\bar{b}$ is the best decay mode for both channels. When we come to different channels, $e^-p \to \nu_e \bar{t} \to \nu_e H\bar{q}$ is much better than $e^-p \to \nu_e Hb$ channels by almost ten times. Finally, we use our best limits in $H \to b\bar{b}$ decay modes for $e^-p \to \nu_e \bar{t} \to \nu_e H\bar{q}$ channel, and we get 0.0134% for $\mathrm{Br}(t \to qH)$ as our result at 14 TeV LHeC with 200 fb^{-1} luminosity.

IV. SUMMARY AND CONCLUSION

In this paper, we investigated the anomalous FCNC Yukawa interactions between the top quark, the Higgs boson, and either an up or charm quark ($tqH, q = u, c$). We choose the channel $e^-p \to \nu_e \bar{t} \to \nu_e H\bar{q}$ with $q = u, c$ and the channel $e^-p \to \nu_e Hb$, where both channels are induced by the charged current interaction through e^-p collision at the LHeC. We consider the $H \to \gamma\gamma, b\bar{b}$, and $\tau^+\tau^-$ decay modes. From the results, we can see that the flavor changing couplings κ_{tuH} can be probed to be minimal as 0.0162 (0.0136) for the 95% C.L. limits in the $e^-p \to \nu_e \bar{t} \to \nu_e H\bar{q}$ channel with the $H \to b\bar{b}$ decay mode, which

corresponds to the branching ratios $\mathrm{Br}(t \to qh) = 1.34(0.947) \times 10^{-4}$ at 14 TeV LHeC with 200(3000) fb^{-1} luminosity. From CMS and ATLAS collaborations, we get the most stringent constraint of $\mathrm{Br}(t \to cH) < 0.56\%$, $\mathrm{Br}(t \to uH) < 0.45\%$ at 95% C.L. [20]. Thus, we can see that our results show a strong (above 30 times) improvement from experiments. When comparing with the other phenomenological studies, we can see that the LHeC sensitivity results for $\mathrm{Br}(t \to qH)$ are smaller than the sensitivity limits of LHC as $\mathrm{Br}(t \to qH) < 5(2) \times 10^{-4}$ with an integrated luminosity of 300 (3000) fb^{-1} at $\sqrt{s} = 14$ TeV [26]. Furthermore, our results are comparable with those of other studies, such as Refs. [24,25]. For example, Ref. [24] obtains the sensitivity bound of about 0.1–0.3% through different search channels for an integrated luminosity of 100 fb^{-1} at the $\sqrt{s} = 13$ TeV LHC data.

ACKNOWLEDGMENTS

H. S. acknowledges Fawzi Boudjema for his warm hospitality at Laboratoire d'Annecy-le-Vieux de Physique Théorique (LAPTh). This project was supported by the National Natural Science Foundation of China (Grant No. 11205070), the Shandong Province Natural Science Foundation (Grant No. ZR2012AQ017), the Fundamental Research Funds for the Central Universities (Grant No. DUT15LK22), and China Scholarship Council (Grant CSC No. 201406065026).

[1] G. Aad *et al.* (ATLAS Collaboration), Observation of a new particle in the search for the standard model Higgs boson with the ATLAS detector at the LHC, Phys. Lett. B **716**, 1 (2012).
[2] S. Chatrchyan *et al.* (CMS Collaboration), Observation of a new boson at a mass of 125 GeV with the CMS experiment at the LHC, Phys. Lett. B **716**, 30 (2012).
[3] S. Glashow, J. Iliopoulos, and L. Maiani, Weak interactions with lepton-hadron symmetry, Phys. Rev. D **2**, 1285 (1970).
[4] A. Dedes, M. Paraskevas, J. Rosiek, K. Suxho, and K. Tamvakis, Rare top-quark decays to Higgs boson in MSSM, J. High Energy Phys. 11 (2014) 137.
[5] J. Cao, C. Han, L. Wu, J. M. Yang, and M. Zhang, SUSY induced top quark FCNC decay $t \to cH$ after run I of the LHC, Eur. Phys. J. C **74**, 3058 (2014).
[6] J. J. Cao, G. Eilam, M. Frank, K. Hikasa, G. L. Liu, I. Turan, and J. M. Yang, SUSY-induced FCNC top-quark processes at the Large Hadron Collider, Phys. Rev. D **75**, 075021 (2007).
[7] J. Cao, Z. Heng, L. Wu, and J. M. Yang, R-parity violating effects in top-quark FCNC productions at the LHC, Phys. Rev. D **79**, 054003 (2009).
[8] D. Lopez-Val, J. Guasch, and J. Sola, Single top-quark production by strong and electroweak supersymmetric flavor-changing interactions at the LHC, J. High Energy Phys. 12 (2007) 054.
[9] G. Eilam, A. Gemintern, T. Han, J. M. Yang, and X. Zhang, Top-quark rare decay $t \to ch$ in R-parity-violating SUSY, Phys. Lett. B **510**, 227 (2001).
[10] T.-J. Gao, T.-F. Feng, F. Sun, H.-B. Zhang, and S.-M. Zhao, Top-quark decay to a 125 GeV Higgs in BLMSSM, Chin. Phys. C **39**, 073101 (2015).
[11] J. M. Yang, B.-L. Young, and X. Zhang, Flavor-changing top-quark decays in R-Parity violating SUSY, Phys. Rev. D **58**, 055001 (1998).
[12] K.-F. Chen, W.-S. Hou, C. Kao, and M. Kohda, When the Higgs meets the top: search for $t \to ch^0$ at the LHC, Phys. Lett. B **725**, 378 (2013).
[13] S. Bejar, J. Guasch, and J. Sola, Higgs boson flavor-changing neutral decays into top quark in a general two-Higgs-doublet model, Nucl. Phys. **B675**, 270 (2003).
[14] G. Eilam, J. L. Hewett, and A. Soni, Rare decays of the top quark in the standard and two Higgs doublet models, Phys. Rev. D **44**, 1473 (1991); Phys. Rev. D **59**, 039901 (1998).
[15] C. Kao, H.-Y. Cheng, W.-S. Hou, and Joshua Sayre, Top decays with flavor changing neutral Higgs interactions at the LHC, Phys. Lett. B **716**, 225 (2012).
[16] A. Azatov, M. Toharia, and L. Zhu, Higgs mediated FCNCs in warped extra dimensions, Phys. Rev. D **80**, 035016 (2009).
[17] S. Casagrande, F. Goertz, U. Haisch, M. Neubert, and T. Pfoh, The custodial Randall-Sundrum model: from precision tests to Higgs physics, J. High Energy Phys. 09 (2010) 014.
[18] R. Gaitan, O. Miranda, and L. Cabral-Rosetti, Rare top-quark and Higgs boson decays in alternative left-right symmetric models, Phys. Rev. D **72**, 034018 (2005); Rare top-quark decays in extended models, AIP Conf. Proc. **857**, 179 (2006).
[19] B. Yang, N. Liu, and J. Han, Top-quark FCNC decay to 125 GeV Higgs boson in the littlest Higgs model with T-parity, Phys. Rev. D **89**, 034020 (2014).
[20] CMS Collaboration, Searches for heavy Higgs bosons in two-Higgs-doublet models and for $t \to ch$ decay using multilepton and diphoton final states in pp collisions at 8 TeV, Phys. Rev. D **90**, 112013 (2014); CMS Collaboration, Report No. CMS-PAS-HIG-13-034, 2014, http://cds.cern.ch/record/1666526/files/HIG-13-034-pas.pdf.
[21] G. Aad *et al.* (ATLAS Collaboration), Search for top-quark decays $t \to qH$ with $H \to \gamma\gamma$ using the ATLAS detector, J. High Energy Phys. 06 (2014) 008.

[22] ATLAS Collaboration, Report No. ATLAS-CONF-2013-081, 2013.
[23] D. Atwood, S. K. Gupta, and A. Soni, Constraining the flavor changing Higgs couplings to the top quark at the LHC, J. High Energy Phys. 10 (2014) 57.
[24] A. Greljo, J. F. Kamenik, and J. Kopp, Disentangling flavor violation in the top-Higgs Sector at the LHC, J. High Energy Phys. 07 (2014) 046.
[25] L. Wu, Enhancing the production from top-Higgs FCNC couplings, J. High Energy Phys. 02 (2015) 061.
[26] K. Agashe *et al.* (Top Quark Working Group Collaboration), Snowmass 2013 top-quark working group report, arXiv:1311.2028.
[27] M. Gorbahn and U. Haisch, Searching for $t \to c(u)h$ with dipole moments, J. High Energy Phys. 06 (2014) 033.
[28] C. Zhang and F. Maltoni, Top-quark decay into Higgs boson and a light quark at next-to-leading order in QCD, Phys. Rev. D **88**, 054005 (2013).
[29] Y. Wang, F. P. Huang, C. S. Li, B. H. Li, D. Y. Shao, and J. Wang, Constraints on flavor-changing neutral-current Htq couplings from the signal of tH associated production with QCD next-to-leading order accuracy at the LHC, Phys. Rev. D **86**, 094014 (2012).
[30] J. A. Aguilar-Saavedra, Top flavor-changing neutral interactions: theoretical expectations and experimental detection, Acta Phys. Pol. B **35**, 2695 (2004).
[31] B. Altunkaynak, W.-S. Hou, C. Kao, M. Kohda, and B. McCoy, Flavor changing heavy Higgs interactions at the LHC, arXiv:1506.00651.
[32] N. Craig, J. A. Evans, R. Gray, M. Park, S. Somalwar, S. Thomas, and M. Walker, Searching for $t \to ch$ with multileptons, Phys. Rev. D **86**, 075002 (2012).
[33] C. S. Li, R. J. Oakes, and T. C. Yuan, QCD corrections to $t \to W^+ b$, Phys. Rev. D **43**, 3759 (1991).
[34] W.-S. Hou, Tree level $t \to ch$ or $h \to t\bar{c}$ decays, Phys. Lett. B **296**, 179 (1992).
[35] S. Khatibi and M. M. Najafabadi, Probing the anomalous FCNC interactions in top-Higgs final state and charge ratio approach, Phys. Rev. D **89**, 054011 (2014).
[36] R. Placakyte (H1 and ZEUS Collaborations), Parton distribution functions, arXiv:1111.5452.
[37] K. A. Olive *et al.* (Particle Data Group), The review of particle physics, Chin. Phys. C **38**, 090001 (2014).
[38] J. Pumplin, D. R. Stump, J. Huston, H. L. Lai, P. M. Nadolsky, and W. K. Tung, New generation of parton distributions with uncertainties from global QCD analysis, J. High Energy Phys. 07 (2002) 012; D. Stump, J. Huston, J. Pumplin, W.-K. Tung, H. L. Lai, S. Kuhlmann, and J. F. Owens, Inclusive jet production, parton distributions, and the search for new physics, J. High Energy Phys. 10 (2003) 046.
[39] J. L. Abelleira Fernandez (LHeC Study Group Collaboration), A Large Hadron Electron Collider at CERN: report on the physics and design concepts for machine and detector, J. Phys. G **39**, 075001 (2012).
[40] J. L. Abelleira Fernandez *et al.*, Report No. CERN-LHeC-Note-2012-004-GEN, 2012.
[41] J. Alwall, M. Herquet, F. Maltoni, O. Mattelaer, and T. Stelzer, MadGraph 5: going beyond, J. High Energy Phys. 06 (2011) 128.
[42] C. Duhr, https://feynrules.irmp.ucl.ac.be/wiki/HiggsEffectiveTheory, 2011.
[43] G. Aad *et al.* (ATLAS Collaboration), Measurement of isolated-photon pair production in pp collisions at $\sqrt{s} =$ 7 TeV with the ATLAS detector, J. High Energy Phys. 01 (2013) 086.
[44] S. Chatrchyan *et al.* (CMS Collaboration), Identification of b-quark jets with the CMS experiment, J. Instrum. **8**, P04013 (2013).
[45] M. Köksal and S. C. Inan, Anomalous $tq\gamma$ couplings in γp collision at the LHC, Adv. High Energy Phys. **2014**, 935840 (2014).
[46] H. Sun, Probe anomalous $tq\gamma$ couplings through single top photoproduction at the LHC, Nucl. Phys. **B886**, 691 (2014).